Journal of Alloys and Compounds 649 (2015) 1300–1305

Contents lists available at ScienceDirect

Journal of Alloys and Compounds

journal homepage: http://www.elsevier.com/locate/jalcom

Enhanced magnetic response and metallicity in AB stacked bilayer graphene via Cr-doping

Jyoti Thakur [a], Manish K. Kashyap [a, *], Hardev S. Saini [b], Ali H. Reshak [c, d]

[a] Department of Physics, Kurukshetra University, Kurukshetra 136119, Haryana, India
[b] Department of Physics, Panjab University, Chandigarh 160014, India
[c] New Technologies – Research Centre, University of West Bohemia, Univerzitni 8, 306 14 Pilsen, Czech Republic
[d] Center of Excellence Geopolymer and Green Technology, School of Material Engineering, University Malaysia Perlis, 01007 Kangar, Perlis, Malaysia

ARTICLE INFO

Article history:
Received 3 July 2015
Received in revised form
20 July 2015
Accepted 25 July 2015
Available online 29 July 2015

Keywords:
Bilayer graphene
DFT
PAW
FPLAPW
Spintronics

ABSTRACT

First-principles study for the electronic and magnetic properties of Cr atom doping in lower layer of AB bernal stacked bilayer graphene (BLG) is presented. This doping is analysed in three different configurations; (i) Hollow type (above the centre of C hexagon), (ii) Top-type (directly on the top of any C atom) and (iii) Bridge type (mid point of any C–C bond). It has been observed that the doping of Cr atom enlarges the interlayer spacing in BLG as compared to pure one. The Top-type (T-type) doping is found to be most stable energetically. The doping of Cr atom in all configurations generates the large spin polarization and induces the appreciable magnetic moment. Half metallicity has been obtained in Hollow type (H-type) doping with a suitable band gap of 0.28 eV in minority spin channel. The origin of magnetism has been identified via interactions of *3d*-states of doped Cr atom with *p*-states of inequivalent C atoms present in the vicinity of doping site. The electron densities plots also confirm the metallic nature of Cr-doped BLG. Our results reveal that the resultant BLG has potential for futuristic applications such as high frequency transistors, spintronics, photodetectors and energy resources.

1. Introduction

Graphene, a two-dimensional (2D) honeycomb monolayer sheet was isolated for the first time from graphite in 2004. During last decade, it has attracted immense research attentions due to its amazing electronic, magnetic and transport properties [1,2] e.g. anamalous quantized Hall effect [3,4], ultra-high mobility, carrier density controllable by external means [5], ballistic transport at room temperature and high elasticity [6]. An intrinsic graphene possesses zero band gap as its valance and conduction bands touch at the Dirac point [7], creating an obstruction for its use in nano-electronic devices. As a result, tuning or opening of its band gap becomes crucial for technological applications of graphene. Several strategies are presently being pursed to tune band gap of graphene monolayer both theoretically and experimentally such as surface adsorption, defects created by irradiating high energy electrons or ions [8], rotating carbon atoms at specific angles to form stone wales type defects [9–11], patterning bilayer or even multilayer graphene, utilizing graphene–substrate interaction [12], applying an external electric field to bilayer graphene [13,14] etc. Generally, local magnetic moments [15] and long-range magnetic coupling [16,17] are considered to be liable for observed high temperature magnetism in carbon based nanomaterials [18].

Bilayer graphene (BLG) typically can be found in three configurations *viz.* (i) twisted ones, where the two layers are rotated relative to each other, (ii) graphitic Bernal stacked (AB stacking) where half the atoms in one layer lie atop of half the atoms in other and (iii) identical stacked (AA stacking) with all the atom of one layer lie atop of all atoms in other layer [19]. Stacking order and orientation govern the optical and electronic properties of bilayer graphene. Experimentally, few layer graphene films were synthesized by exfoliation and cleavage methods [20,21]. BLG is gapless semimetal [22,23] with a linear Dirac type dispersion around the Fermi energy (E_F) [24] just similar to single layer graphene (SLG). Ohta et al. [25] synthesized the bilayer graphene thin film deposited on insulating silicon carbide and reported their electronic band structure using angle-resolved photoemission spectroscopy. Although, BLG has many comparable physical properties as that of SLG but there still exists small differences. In BLG, low energy excitation is one of the characteristics of massive chiral fermions

* Corresponding author.
E-mail addresses: manishdft@gmail.com, mkumar@kuk.ac.in (M.K. Kashyap).

http://dx.doi.org/10.1016/j.jallcom.2015.07.241
0925-8388/

unlike Dirac fermions in SLG [1,2]. In addition, small low energy gap in BLG can be tuned easily by breaking the symmetry between layers [26]. Low electrical noise in BLG provides exciting frontiers in low-noise applications [27]. Bilayer graphene displays the anomalous quantum Hall effect and excitonic condensation [28] which make it a promising candidate for optoelectronic and nano-electronic applications. Due to these exotic properties, BLG have received a lot of attentions from researchers in fundamental nanoscience, microelectonics and spintronics.

In contrast to SLG, vacancies, adatom defects, edge effects, chemical and substitutional doping can magnetize BLG. Theoretically, Mao et al. [29] investigated Mn doping in BLG and found a high spin polarized state suitable for spintronic applications. The electronic and magnetic properties of an adatom (Na, Cu or Fe) on bilayer graphene were studied by Nafday and Dasgupta [30]. They found the stable magnetism via Cu and Fe adsorption and weak magnetism by Na adsorption. Gong et al. [31] found that intercalation of C and N atoms in BLG induces magnetization but O-intercalated BLG is non-magnetic. Intrinsic defects, including Stone Wales defects and atom vacancy (H and T vacancy) were studied by Li et al. [32]. Fujimoto and Saito [33] investigated energetics and electronic structure of B- and N-doped BLG with AA as well as AB stacking patterns using ab-initio first principles calculations. They found that B- and N-doped BLG in AB stacking exhibit p-type and n-type semiconducting properties, respectively.

To the best of our knowledge, the case of single Cr-doping in BLG has not been considered till date. However the similar case of Mn-doping is reported [29] in which magnetism is generated to significant amount. This motivated us to carry out first principles calculations to study the electronic and magnetic properties of BLG doped with Cr atom in lower layer. All possible configurations of this doping i.e. (i) Hollow (H-type) (ii) Top (T-type) and (iii) Bridge (B-type) are planned to be considered for this work. The other aim of present investigation is to explore the changes observed in spin electronic and magnetic properties of BLG by single Cr-doping in all possible configurations. Furthermore, it has been shown that Cr doped magnetic/superconducting materials show a huge potential for the photo induced nonlinear optics recently [34,35]. This justifies the importance of studying Cr-doping in BLG for nonlinear optics as well.

2. Theoretical details

We consider only BLG with AB (bernal) stacking [36,37] for the present calculations. AA stacking is avoided due to unfavoured energetics [19]. We have introduced three types of doping of Cr atom in lower layer of BLG i.e. H type (above the centre of hexagon of C atoms), T-type (directly on the top of any C atom), B-type (mid point of any C–C bond). The ($4 \times 4 \times 1$) super cells have been constructed to dope Cr atom in all studied configurations. A vacuum layer of 20 Å thickness in the z-direction is inserted to avoid the interlayer interaction due to periodic boundary conditions. For structural relaxation, we have carried out all calculations using density functional theory [38] (DFT) approach as implemented in Vienna Ab-initio Simulation Package (VASP) [39,40]. The generalized gradient approximation (GGA) under Perdew–Burke–Ernzerhof (PBE) [41] parametrization was used to construct exchange-correlation (XC) potentials. The core electron interaction was described using projected augmented wave (PAW) method. The cut off energy for plane waves was set to be 610 eV. A $9 \times 9 \times 1$ Monkhorst-Pack grid was used for the sampling of the Brillouin zone during geometrical optimization. Conjugate gradient (CG) algorithm [42] was selected to relax present systems. All the internal coordinates were allowed to be relaxed until calculated Hellmann Feymann force on each atom became smaller than 0.02 eV $Å^{-1}$.

After relaxation, final electronic structure calculations were performed using the full-potential linearized augmented plane-wave (FPLAPW) [43] method within GGA as implemented in WIEN2k package [44]. In FPLAPW calculations, the core states were treated fully relativistically whereas for the valence states, a scalar relativistic approach was used. The radii of Muffin-Tin (MT) sphere (R_{MT}) for various atoms were taken in the present calculations such as to ensure the nearly touching sphere. The plane wave cut off parameters were decided by $R_{mt}k_{max} = 7$ (where k_{max} is the largest wave vector of the basis set) and $G_{max} = 12$ a.u.$^{-1}$ for fourier expansion of potential in the interstitial region. Additionally, valence electronic wavefunctions inside the MT sphere were expanded upto $l_{max} = 10$. The k-space integration was carried out using the modified tetrahedron method [45] with a k-mesh of $11 \times 11 \times 1$ for self-consistency.

3. Result and discussion

As a first step, the $4 \times 4 \times 1$ supercell was chosen to simulate the relaxed structures for (i) Hollow (H-type) (ii) Top (T-type) and (iii) Bridge (B-type) doping of Cr atom in pristine BLG. The top and side views of these dopings along with pristine BLG are depicted in Figs. 1 and 2, respectively. The distance between upper and lower layers of graphene in relaxed structure after doping increases in the order.

T-type > B-type > H-type

The ground state energies of relaxed structures as calculated by VASP are also found in the same order as shown in Table 1. The relaxed lattice parameters for pure and doped BLG along with various bond lengths between Cr atom and various C atoms are also depicted in Table 1. To confirm, the structure stability in each configuration, the ground state energies for these were calculated once again using FPLAPW method as incorporated in WIEN2k. This method also predicts the same order of structural stability as that of VASP i.e. T-type doping in BLG is most favourable energetically stable. Concentrating on common bond in three configurations, we found that bond length for Cr–C_1 comes out to be minimum in T-type doping confirming the strongest covalent bond among all. On relaxation, the pristine BLG has common C–C bond lengths of 1.420 Å in both layers. Further even on doping of any type, the C–C bond length (1.420 Å) after relaxation in upper layer remains preserved. However in lower layer, the C ring containing doping gets distorted and deviates from its regular hexagonal shape. Now all the C–C bond lengths appear to be different (Fig. 3). The various C–Cr bond lengths are mentioned in Fig. 3/Table 1.

Fig. 4 manifests the calculated spin-resolved total density of states (DOS) of pure and doped BLG. Pure BLG manifests the symmetrical DOS in both spin channels and this property just resembles with SLG [46]. On doping in BLG, Cr atom plays a significant role to tune the Fermi level (E_F). In H-type configuration, asymmetrical DOS among majority and minority spin channels (MAC and MIC) in the vicinity of E_F leads to transition from semimetallic to half metallic state of BLG. An appreciable band gap of 0.28 eV has been observed in this system for MIC. Opening up of band gap in one spin channel increases the potential of doped graphene in spin transport. The similar tuning of band gap in semimetallic BLG-BN heterostructures was reported by Ramasubramaniam [47]. He pointed out that these heterostructures could provide a viable route to graphene based electronic devices. Thus we can claim that H-type Cr-doped BLG may be a good candidate for graphene based spintronics.

In T-type and B-type, there is asymmetrical DOS present among both channels in the vicinity of E_F which shifts BLG in metallic state.

There exists some theoretical evidences [29,31,32] supporting our predictions which manifests the similar transition of BLG on doping. The spin-polarization P of a material [48–50] can be calculated by,

$$P = \frac{N_{\uparrow}(E_F) - N_{\downarrow}(E_F)}{N_{\uparrow}(E_F) + N_{\downarrow}(E_F)} \quad (1)$$

where $N_{\uparrow}(E_F)$ and $N_{\downarrow}(E_F)$ are the spin dependent density of states of majority (↑) and minority (↓) spin electrons at the E_F, respectively.

The maximum value of spin polarization (100%) was observed in H-type, suggesting a promising way for transporting spin polarized currents in spin based quantum information devices [51–53] within BLG. The other two types of doping in BLG *viz.* T-type and B-type also possess spin polarizations of 78.3% and 63.0%, respectively (Table 2), which are also appreciable for spin transport.

To have a better understanding of contribution of individual atom for various energy bands in doped BLG, partial spin resolved density of states (PDOS) is depicted in Fig. 5. In H-type doped BLG, we have noticed that 3d states of doped Cr atom have a pivot role in generation of DOS in the vicinity of E_F. Not only Cr atom, but also nearest neighbour C atoms to Cr atom are responsible for shifting of the DOS near the E_F in both MAC and MIC. The C atoms away from doping site (C_{far}) represent almost identical DOS in the vicinity of E_F, confirming that they have no role to decide any spin conduction. Similar explanation may be given for explaining DOS of T-type and B-type doping.

Pure BLG possess zero magnetic moment. But on doping of Cr atom in BLG, many C atoms become non-equivalent. The Cr atom and non-equivalent C atoms with spin polarized DOS induce the magnetic moment on BLG as shown in Table 2. We have found the magnetic moments of 1.99 μ_B, 1.23 μ_B and 1.10 μ_B for doped graphene in H-type, T-type and B-type configurations, respectively. The maximum magnetic moment in H type doping is the consequence of 100% spin polarized DOS at E_F as the magnetic moment is proportional to the difference of DOS in two spin channels. The other two types of doping (i.e. T-type and B-type) possess lower spin polarizations as the difference between majority and minority spin DOS is not as significant as in case of H-type. This leads to lower value of magnetic moments in these cases.

The other C atoms, which are away from doped site do not possess significant magnetic moments. However, some magnetic moment is found to be distributed evenly in the interstitial regions among C atoms, which is also the case for Cu doped transition metal dichaclogenides; MoS_2 single layer. This indicates that the magnetic moment distributed over the interstitial regions should also have significant contribution and cannot be ignored [54].

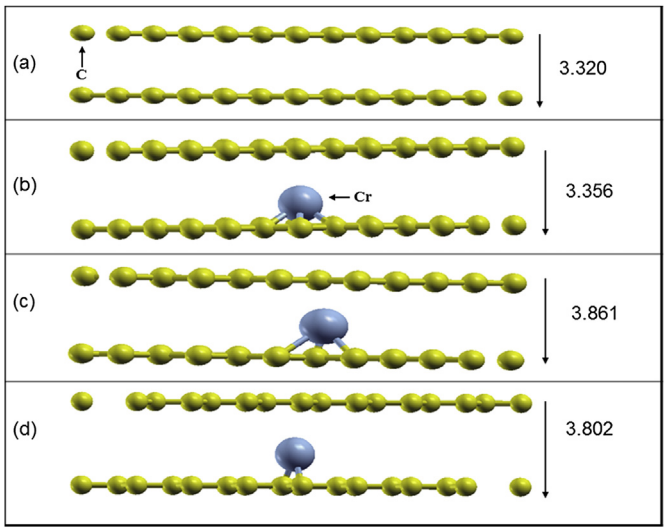

Fig. 2. Side view of all studied nanosystems; (a) pure BLG, (b) H-type, (c) T-type and (d) B-type, Cr-doping in lower layer of BLG.

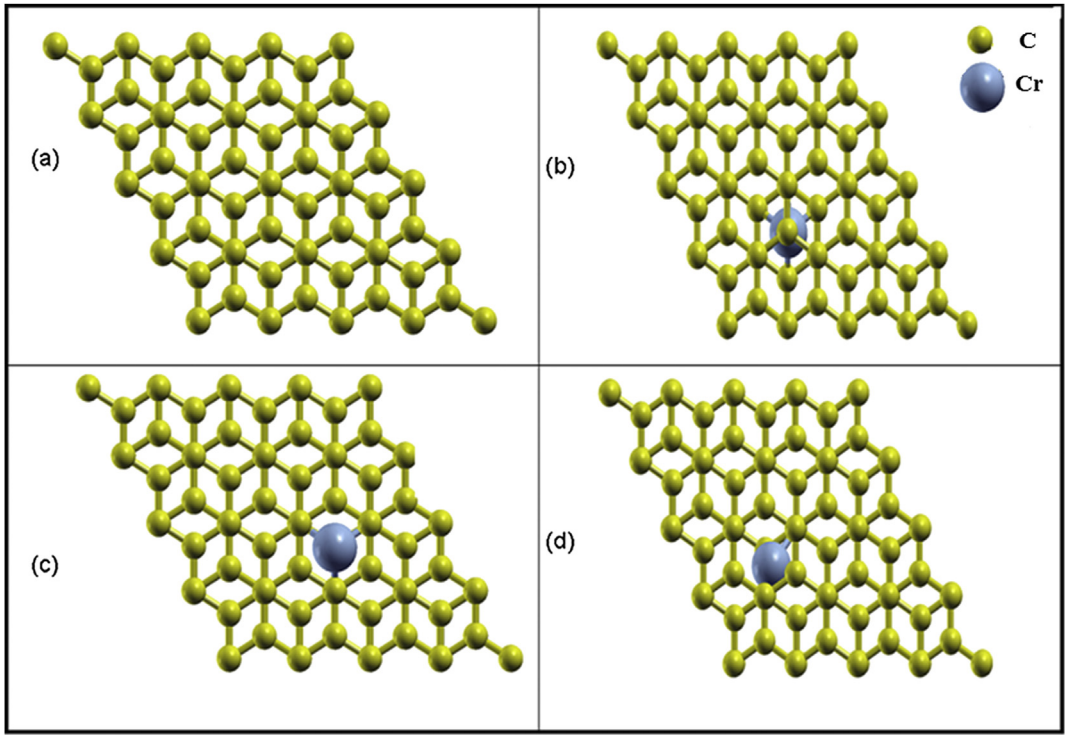

Fig. 1. Top view of all studied nanosystems; (a) pure BLG, (b) H-type, (c) T-type and (d) B-type, Cr-doping in lower layer of BLG.

Table 1
Calculated relaxed lattice parameters, bond lengths between doped Cr atom and its nearest C atoms, and layer spacing of doped system.

Bilayer doping configuration	Lattice parameters (Á)	Bond length (Á)	Spacing (Á)	Ground state energy (eV) (WIEN2k)	Ground state energy (eV) (VASP)
Hollow (H-type)	a = b = 9.77 c = 19.28	Cr–C_1 = 1.777 Cr–C_3 = 1.601 Cr–C_5 = 1.395	3.356	−94,833.26	−93,456.37
Top (T-type)	a = b = 9.77 c = 19.93	Cr–C_1 = 1.679 Cr–C_2 = 1.882 Cr–C_6 = 1.336	3.861	−94,866.13	−93,478.62
Bridge (B-type)	a = b = 9.77 c = 19.64	Cr–C_1 = 1.733 Cr–C_2 = 1.535	3.803	−94,847.59	−93,465.96

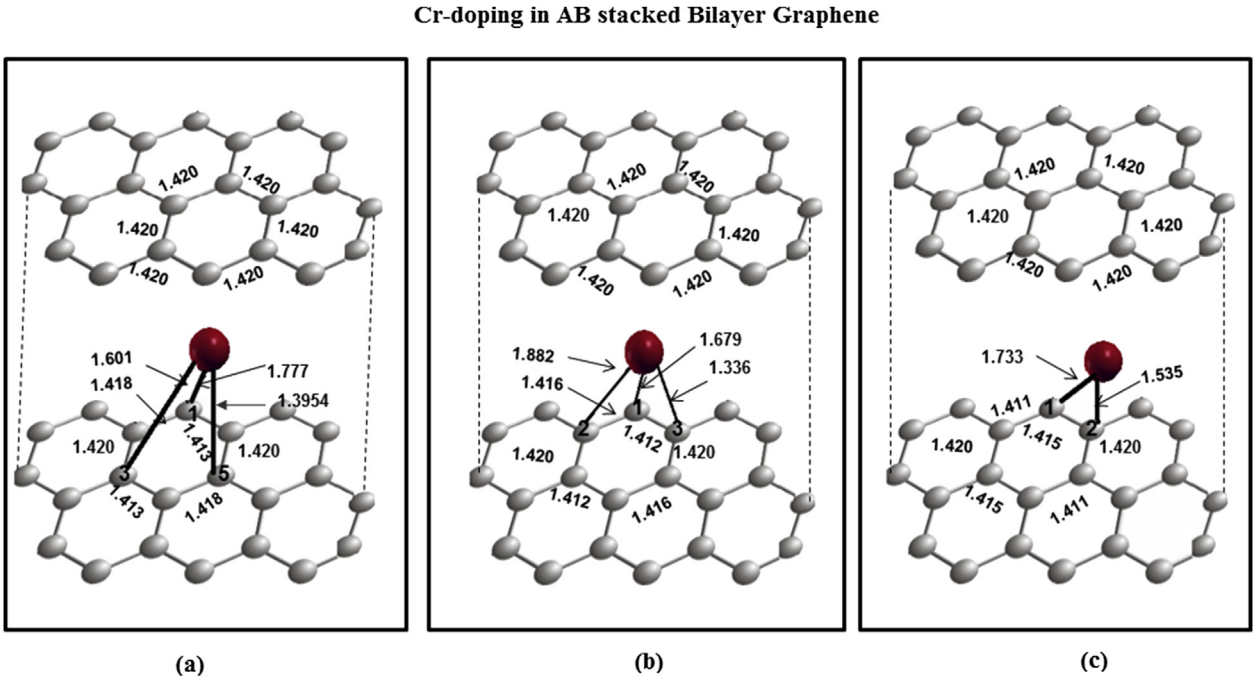

Fig. 3. Relaxed bond lengths (Á) for (a) H-type, (b) T-type and (c) B-type, Cr-doping in lower layer of BLG.

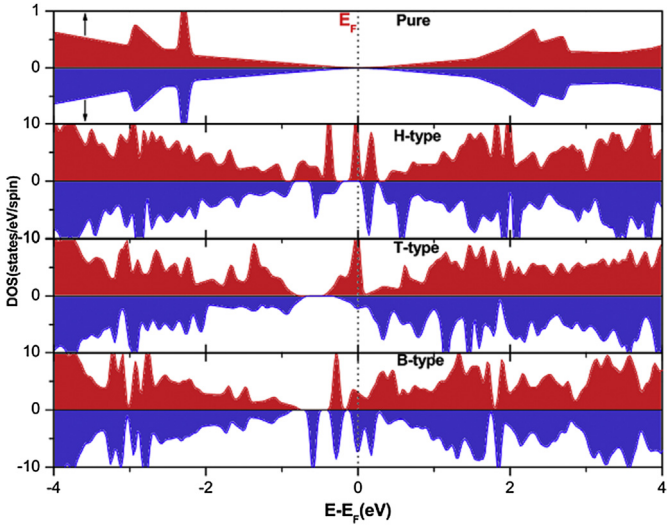

Fig. 4. Calculated spin-resolved total density of states (DOS) of pure BLG, H-type, T-type and B-type, on Cr-doping.

In order to cross verify the metallic response, the spin dependent valence electronic densities have been analysed for all type of dopings in Fig. 6. It is evident that pure BLG is covalently hybridized with electronic charge, equally shared between p-orbitals of two adjacent atoms in two spin channels. However, the picture becomes different on doping. Now in H-type doping (Fig. 6(b)), the bonding of Cr atom with 3 alternate C atoms of hexagon (shown in Fig. 3(a)) in lower layer of BLG results the charge sharing in a wider area. But Cr atoms have mainly majority electrons which lead to spin polarization at E_F and thus semiconducting behaviour for minority spin observed. On the other hand, the doped Cr atom is linked with 3/2 adjacent C atoms of lower layer in (i) T-type/(ii)B-type configurations (Fig. 6(c) and (d)). The charge sharing is not

Table 2
Spin resolved density of states of majority (↑) and minority (↓) spin electrons at E_F, spin polarizations (P), electronic band gaps (E_g), metallic states and total magnetic moments of pure and doped BLG.

Bilayer graphene	$N_\uparrow(E_F)$	$N_\downarrow(E_F)$	P (%)	E_g (eV)	State	M_{tot} (μ_B)
Pure	0.00	0.00	–	–	Semi-metallic	0.00
H-type	6.16	0.00	100.0	0.28	Half-metallic	1.99
T-type	9.98	1.21	78.3	–	Metallic	1.23
B-type	5.24	1.15	63.0	–	Metallic	1.10

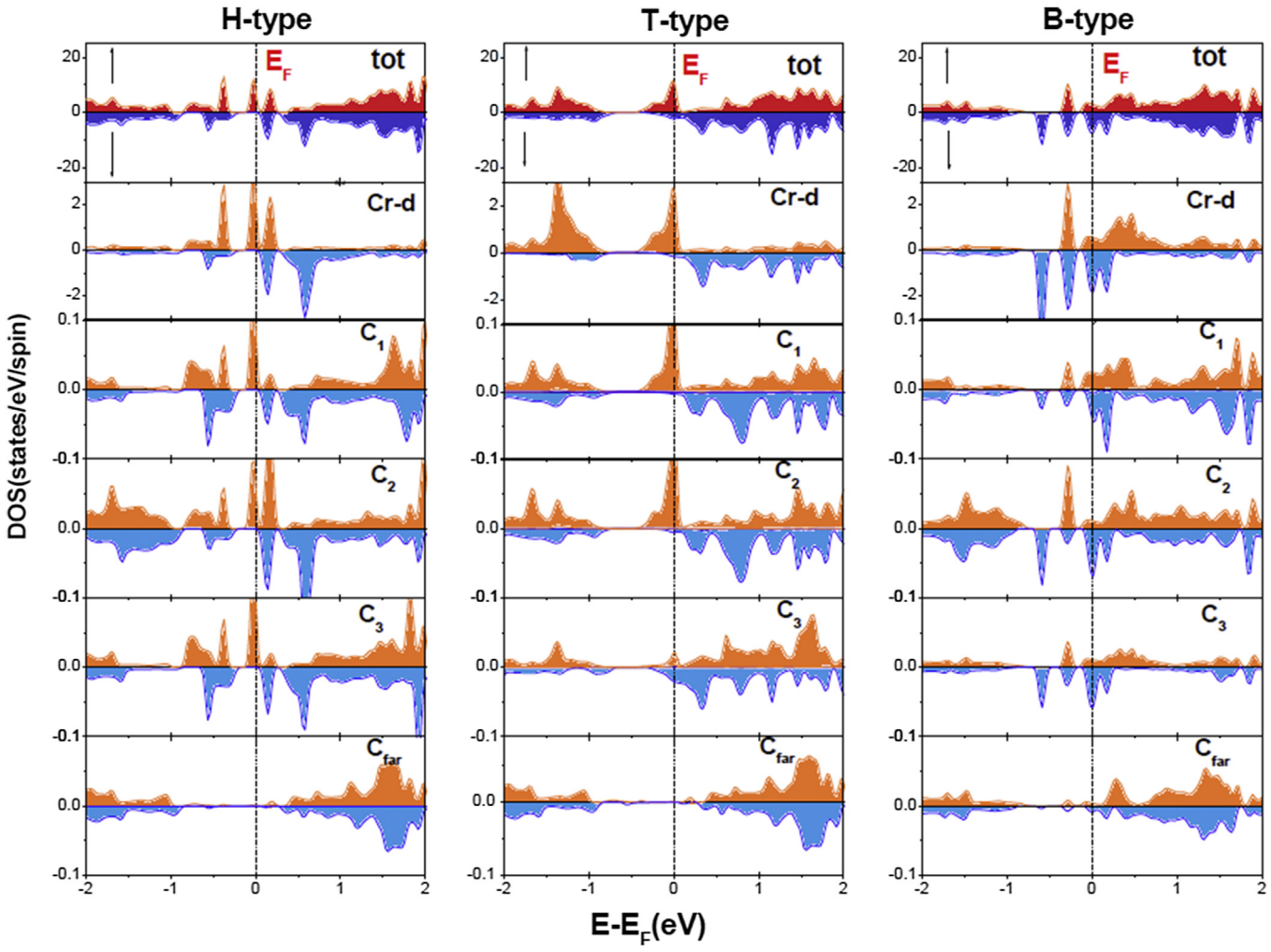

Fig. 5. Partial density of states (PDOS) of Cr-doped graphene in H-type, T-Type and B-type configurations.

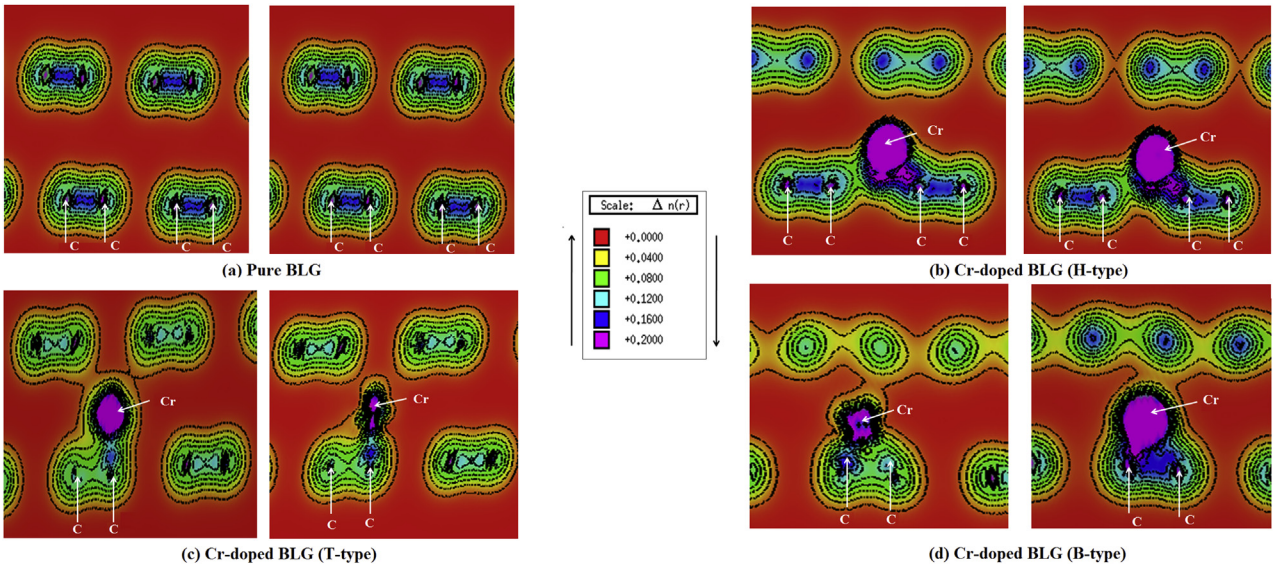

Fig. 6. Spin polarized valence electron charge densities, n(r) in a plane perpendicular to both graphene layers in case of pure BLG and for plane containing doped Cr-atom and both graphene layers in case of Cr-doped BLG in units of e/a.u.^{3}.

only limited to lower layer but also gets extended in upper layer as well. Due to interactions of Cr atom with C atoms of both layers, the total electronic charge get dispersed over E_F and its vicinity which leads the resultant nanomaterial in complete metallic state.

4. Conclusions

The electronic and magnetic properties of Cr doped BLG in lower layer within three types of configurations (H-, T- and B-type) have been studied using density functional theory (DFT) approach. The PAW method within VASP and FPLAPW method within WIEN2k were tested to verify the stability of Cr-doping in BLG in these configurations. Both approaches predict that the T-type doping in BLG is highest stable among others. On Cr doping, the electronic properties and magnetic response of BLG get modified drastically. The zero band gap of BLG gets closed and significant magnetic moment starts appearing on Cr-doping. The magnetic moment is mainly contributed by doped Cr atom with appreciable contributions from nearby C atoms as well. Valence electronic density analysis demonstrates that the charge transfer from doped Cr atom to C atom of BLG results in shifting of DOS at E_F and leads to a transition from semimetallic to half-metallic or metallic state. A complete spin polarization in H-type and appreciable 78.3%/63.0% spin polarization in T-type/B-type configurations makes resultant BLG most probable nanomaterial for the development of nanoscale devices for spintronic applications, spin filters and injector devices. Moreover, the potential of Cr-doping [34,35] in BLG for nonlinear optical response cannot be ignored and has to be explored definitely.

Acknowledgements

The computational facilities used for the work are supported by UGC, INDIA, grant no. 41-922/2012 (SR) sanctioned to M. K. Kashyap. H.S. Saini acknowledges UGC, INDIA for providing financial support as Dr. D. S. Kothari post doctoral fellowship. For the author – A. H. Reshak, the result was developed within the CENTEM project, reg. no. CZ.1.05/2.1.00/03.0088, cofunded by the ERDF as part of the Ministry of Education, Youth and Sports OP RDI programme and, in the follow-up sustainability stage, supported through CENTEM PLUS (LO1402) by financial means from the Ministry of Education, Youth and Sports under the "National Sustainability Programme I". Computational resources were provided by MetaCentrum (LM2010005) and CERIT-SC (CZ.1.05/3.2.00/08.0144) infrastructures.

References

[1] A.K. Geim, K.S. Novoselov, Nat. Mater. 6 (2007) 183.
[2] K.I. Bolotin, K.J. Sikes, Z. Jiang, M. Klima, G. Fudenberg, J. Hone, P. Kim, H.L. Stromer, Solid State Commun. 146 (2008) 351.
[3] K.S. Novoselov, A.K. Geim, S.V. Morozov, D. Jiang, Y. Zhang, S.V. Dubonos, I.V. Grigorieva, A.A. Firsov, Science 315 (2007) 1379.
[4] Y. Zhang, Y.W. Tan, H.L. Stromer, P. Kim, Nature 438 (2005) 201.
[5] K.S. Novoselov, A.K. Geim, S.V. Morozov, D. Jiang, Y. Zhang, S.V. Dubonos, I.V. Grigorieva, A.A. Firsov, Science 306 (2004) 666.
[6] C. Lee, X. Wei, J.W. Kysar, J. Hone, Science 321 (2008) 385.
[7] K.S. Novoselov, A.K. Geim, S.V. Morozov, D. Jiang, M.I. Katneslson, I.V. Grigorievia, S.V. Dubonos, A.A. Firsov, Nature 438 (2005) 197.
[8] A.V. Krasheninniov, K. Nordlund, J. Appl. Phys. 107 (2010) 071301.
[9] L. Sun, Q.X. Li, H. Ren, H.B. Su, Q.W. Shi, J.L. Yang, J. Chem. Phys. 129 (2008) 074704.
[10] S.C. Pradhan, J.K. Phadikar, Phys. Lett. A 373 (2009) 1062.
[11] P. Lu, Z. Zhang, W. Guo, Phys. Lett. 373 (2009) 3354.
[12] S.Y. Zhou, G.H. Gweon, A.V. Fedorov, P.N. First, W.A. dee Heer, F. Guinea, A.H. Neto Castro, A. Lanzara, Nat. Mater. 6 (2007) 770.
[13] Y. Zhang, T.T. Tang, C. Girit, Z. Hao, M.C. Martin, A. Zettl, M.F. Crommie, Y.R. Shen, F. Wang, Nature 459 (2009) 820.
[14] M. Khantha, N.A. Cordero, L.M. Molina, J.A. Alonso, L.A. Girifalco, Phys. Rev. B 76 (2004) 073103.
[15] F. Banhart, J. Kotakoski, A.V. Krasheninnikov, ACS Nano 5 (2011) 26.
[16] H.H. Xia, W.F. Li, Y. Song, X.M. Yang, X.D. Liu, M.W. Zhao, Y.Y. Xia, C. Song, T.W. Wang, D.Z. Zhu, J.L. Gong, Z.Y. Zhu, Adv. Mater. 20 (2008) 4679.
[17] I.C. Gerber, A.V. Krasheninnikov, A.S. Foster, R.M. Nieminen, New J. Phys. 12 (2010) 113201.
[18] P. Avouris, Z. Chen, V. Perebenios, Nat. Nanotechnol. 2 (2007) 605.
[19] M. Khantha, N.A. Cordero, L.M. Molina, J.A. Alonso, L.A. Girifalco, Phys. Rev. B 70 (2004) 125422.
[20] A. Reina, X. Jia, J. Ho, D. Nezich, H. Son, V. Bulovic, M.S. Dresselhaus, J. Kong, Nano Lett. 9 (2008) 30.
[21] K.S. Kim, Y. Zhao, H. Jang, S.Y. Lee, J.M. Kim, J.H. Ahn, P. Kim, J.Y. Choi, B.H. Hong, Nature 457 (2009) 706.
[22] E. McCann, V.I. Falko, Phys. Rev. Lett. 96 (2006) 086805.
[23] A.H.C. Neto, F. Guiena, N.M.R. Peres, K.S. Novoselov, A.K. Geim, Rev. Mod. Phys. 81 (2009) 109.
[24] W. Choi, I. Lahiri, R. Seelaboyina, Y.S. Kang, Crit. Rev. Solid State Mater. Sci. 35 (2010) 52.
[25] T. Ohta, A. Bostwick, T. Seyll, K. Horn, E. Rotenberg, Science 313 (2006) 951.
[26] B.R.K. Nanda, S. Satpathy, Phys. Rev. B 80 (2009) 165430.
[27] Y.M. Lin, P. Avouris, Nano Lett. 8 (2008) 2119.
[28] Y. Barlas, R. Cote, J. Lambert, A.H. MacDonald, Phys. Rev. Lett. 104 (2010) 096802.
[29] Y. Mao, J. Zhong, Nanotechnology 19 (2008) 205708.
[30] D. Nafday, T.S. Dasgupta, Phys. Rev. B 88 (2013) 205422.
[31] S.J. Gong, W. Sheng, Z.Q. Yang, J.H. Chu, J. Phys. Condens. Matter. 22 (2010) 245502.
[32] T. Li, X. Tang, Z. Liu, P. Zhang, Phys. E 43 (2011) 1597.
[33] Y. Fujimoto, S. Saito, Surf. Sci. 634 (2015) 57.
[34] N.S. Alzayed, I.V. Kityk, S. Soltan, A. Wojciechowski, A.O. Fedorchuk, G. Lakshminarayana, M. Shahabuddin, J. Alloys Compd. 594 (2014) 60–64.
[35] N.S. Alzayed, I.V. Kityk, S. Soltan, A. Wojciechowski, A.O. Fedorchuk, G. Lakshminarayana, M. Shahabuddin, Phys. E 63 (2014) 180–185.
[36] S. Latil, L. Henrard, Phys. Rev. Lett. 97 (2006) 036803.
[37] J. Charlier, J.P. Michenaud, Phys. Rev. B 46 (1992) 4531.
[38] M. Weinert, E. Wimmer, A.J. Freeman, Phys. Rev. B 26 (1982) 4571.
[39] G. Kresse, J. Furthmüller, Comp. Mater. Sci. 6 (1996) 15.
[40] G. Kresse, J. Furthmüller, Phys. Rev. B 54 (1996) 11169.
[41] J.P. Perdew, K. Burke, M. Ernzehof, Phys. Rev. Lett. 77 (1996) 3865.
[42] R.P. Feynman, Phys. Rev. 56 (1939) 340.
[43] G.K.H. Madsen, P. Blabha, Phys. Rev. B 64 (2001) 195134.
[44] P. Blaha, K. Schwarz, G. Madsen, D.K.J. Luitz, K. Wien, An Augmented Plane Wave Plus Local Orbitals Program for Calculating Crystal Properties, Vienna University of Technology, Austria, 2001. ISBN: 3-9501031-1-2.
[45] P.E. Blöchl, O. Jepsen, O.K. Andersen, Phys. Rev. B 49 (1994) 16223.
[46] A.W. Robertson, B. Montanari, K. He, C.S. Allen, Y.A. Wu, N.M. Harrison, J.H. Warner, ACS Nano 7 (2013) 4495.
[47] A. Ramasubramaniam, Nano Lett. 11 (2011) 1070.
[48] R.J. Soulen Jr., J.M. Byers, M.S. Osofsky, B. Nadgorny, T. Ambrose, S.F. Cheng, P.R. Broussard, C.T. Tanaka, J. Nowak, J.S. Moodera, A. Barry, J.M.D. Coey, Science 282 (1998) 85.
[49] H.S. Saini, M. Singh, A.H. Reshak, M.K. Kashyap, Comp. Mater. Sci. 74 (2013) 114.
[50] M. Singh, H.S. Saini, M.K. Kashyap, J. Mater. Sci. 48 (2013) 1837.
[51] V.M. Karpan, G. Giovannetti, P.A. Khomyakov, M. Talanana, A.A. Starikov, M. Zwierzycki, P.J. Kelly, Phys. Rev. Lett. 99 (2007) 176602.
[52] X.H. Zheng, R.N. Wang, L.L. Song, Z.X. Dai, X.L. Wang, Z. Zeng, Appl. Phys. Lett. 95 (2009) 123109.
[53] W. Sheng, Z. Ning, Z.Q. Yang, H. Guo, Nanotechnology 21 (2010) 385201.
[54] W.S. Yun, J.D. Lee, Phys. Chem. Chem. Phys. 16 (2014) 8990.